Analysis of Torque Ripple Due to Phase Commutation in Brushless dc Machines

Renato Carlson, *Member, IEEE*, Michel Lajoie-Mazenc, and Joao C. dos S. Fagundes

Abstract—**An original analytical study is developed concerning the torque ripple due to phase commutation on brushless dc motors. The results indicate that the relative ripple is independent of current, varies with speed, and may reach 50% of the average torque. The amplitude of the torque ripple and the duration of the commutation are analyzed, showing how this affects the torque-speed curve of the drive. Simulation as well as experimental results that validate the theoretical analysis are presented.**

Introduction

BRUSHLESS dc motors have a trapezoidal back emf waveform and are fed with rectangular stator currents (Fig. 1). Under these conditions, the torque produced is theoretically constant. However, in practice, torque ripple may exist, due to the machine itself but also to the feeding system. The causes of ripple coming from the machine are cogging torque and emf waveform imperfections, and those coming from the supply are current ripple (resulting from the PWM or hysteresis control) and phase current commutation.

Many ways were proposed to attenuate cogging torque, mainly by slot skewing or by changing the magnet's dimensions and positioning [1]-[2]. Emf or static torque imperfections were analyzed, and some original solutions were proposed to overcome them [3]. On the other hand, few studies of ripple due to the supply are available. To our knowledge, only Pillay and Krishnan have shown, using a simulation, that the commutation can introduce significant torque pulsation [4].

Therefore, in order to obtain a better understanding of brushless dc motor behavior, an original analytical study of commutation is proposed in this paper. The evolution of the torque during the current commutation between two phases of the machine is analyzed, and the developed expressions allow a determination of torque ripple due to this commutation. The theoretical analysis is illustrated by simulation and experimental results.

Paper IPCSD 91-86, approved by the Electric Machines Committee of the IEEE Industry Applications Society for presentation at the 1990 Industry Applications Society Annual Meeting, Seattle, WA, October 1-5. Manuscript released for publication June 3, 1991.

R. Carlson and J. C. dos S. Fagundes are with the Department of Electrical Engineering, Universidade Federal do Rio Grande do Sul, Florianopolis, Brazil.

M. Lajoie-Mazenc is with the Laboratoire d'Electrotechnique et d'Electronique Industrielle, Toulouse, France.

IEEE Log Number 9106823.

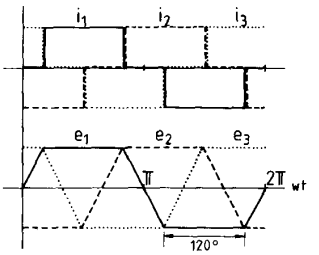

Fig. 1. Currents and back emf waveforms in a brushless dc motor.

Description of the System and General Assumptions

A brushless dc motor drive consists of a permanent magnet machine fed by a current controlled inverter. This is shown in Fig. 2, where the dc supply has been idealized.

There are two levels of current control. The first one determines the phase sequence and the moment of current commutations from one phase to the following one. This control is determined from a rotor position sensor. The second level controls the current amplitude from machine current's sensing and can be done by PWM or by hysteresis.

Usually, the machine currents are directly measured by sensors placed in the ac link between inverter and machine, but with rectangular waveform currents, an image of the phase currents can be obtained by a current sensor placed in the dc link at the inverter input [5], [6]. In the following, these two configurations will be successively examined.

The machine model and the conventions adopted for the study are shown in Fig. 3. Assuming constant self and mutual inductances, the voltage equation is

$$\begin{vmatrix} v_1 \\ v_2 \\ v_3 \end{vmatrix} = \begin{bmatrix} R & 0 & 0 \\ 0 & R & 0 \\ 0 & 0 & R \end{bmatrix} \begin{vmatrix} i_1 \\ i_2 \\ i_3 \end{vmatrix} + \begin{bmatrix} \mathscr{L} & 0 & 0 \\ 0 & \mathscr{L} & 0 \\ 0 & 0 & \mathscr{L} \end{bmatrix} \frac{d}{dt} \begin{vmatrix} i_1 \\ i_2 \\ i_3 \end{vmatrix} + \begin{vmatrix} e_1 \\ e_2 \\ e_3 \end{vmatrix} \tag{1}$$

where $\mathscr{L} = L - M$.

The torque is given by

$$T = \frac{1}{\omega}(e_1 i_1 + e_2 i_2 + e_3 i_3). \tag{2}$$

In order to only show off the torque ripple due to the supply, ideal trapezoidal emf's e_1, e_2, and e_3 (with a 120° constant plateau) are considered.

Control from dc Link Current Sensing

Fig. 4 describes the general structure of the drive with this kind of control. It should be observed that a rectification of

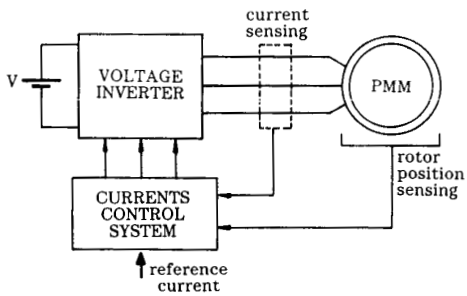

Fig. 2. Schematic of a brushless dc drive.

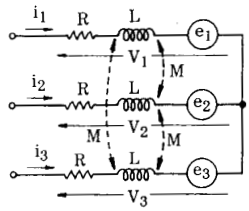

Fig. 3. Machine model and conventions.

the sensed dc link current is needed to get a correct image of the machine current, owing to the current returned by the freewheeling diodes of the inverter. In order to simplify the analysis, an hysteresis control of the current amplitude is adopted.

For this analysis, a very small hysteresis band is considered, and therefore, the current through the winding of the machine between commutations is supposed constant and equal to I.

Commutation Sequences

For this analysis, the commutation of the current from phase 1 to phase 2 is considered. This current transfer is done by switching off $T1$ and by switching on $T2$. Nevertheless, this transfer is not done directly and puts into action the freewheeling diodes. The circuit before this commutation is shown in Fig. 5(a). Immediately after switching off $T1$, the circuit configuration is that of Fig. 5(b). From this point, three different cases can be found that depend on the following operating conditions:

Case a) Current i_1 vanishes at the same time the current i_2 reaches its final value I; the next sequence is then that of Fig. 5(d), and the commutation is finished.

Case b) Current i_1 vanishes before current i_2 reaches its final value; the next sequence is also that of Fig. 5(d), but in this case, the commutation will be achieved only when current i_2 will reach the final value I.

Case c) Current i_2 reaches the value I before current i_1 vanishes; the next sequence is in this case that of Fig. 5(c), where $T2$ and $T6$ are switched off, and three diodes conduct until i_1 vanishes.

Once these three possible sequences are identified, the equations describing the evolution of the phase currents can be established. This will be done neglecting the winding resistance and considering that the emf's remain constant during commutation.

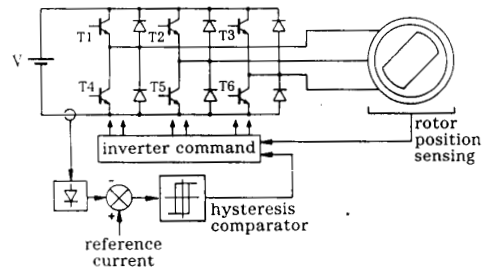

Fig. 4. Schematic of the brushless dc drive with dc link current sensing and hysteresis control.

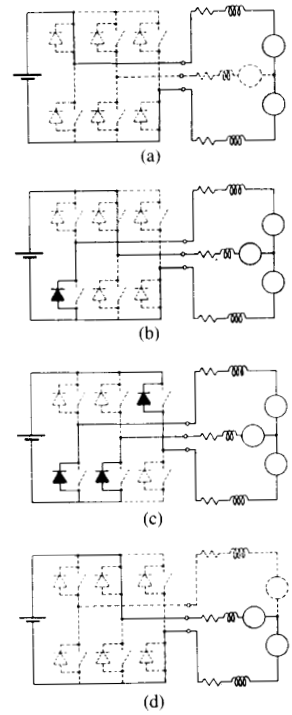

Fig. 5. Commutation sequence: (a) Before commutation; (b) commutation with two switches and one diode conducting; (c) commutation with three diodes conducting; (d) after commutation.

For the sequence of Fig. 5(b), the current derivatives are given by

$$\frac{di_1}{dt} = -\frac{V + 2E}{3\mathscr{L}} \tag{3}$$

$$\frac{di_2}{dt} = +\frac{2(V - E)}{3\mathscr{L}} \tag{4}$$

$$\frac{di_3}{dt} = -\frac{(V - 4E)}{3\mathscr{L}}. \tag{5}$$

Taking the beginning of the commutation as the time

origin, the phase currents are given by

$$i_1 = I - \frac{V + 2E}{3\mathscr{L}}t \tag{6}$$

$$i_2 = \frac{2(V - E)}{3\mathscr{L}}t \tag{7}$$

$$i_3 = -I - \frac{V - 4E}{3\mathscr{L}}t. \tag{8}$$

For the sequence of Fig. 5(c), the current derivatives are given by

$$\frac{di_1}{dt} = -\frac{V + 2E}{3\mathscr{L}} \tag{9}$$

$$\frac{di_2}{dt} = -\frac{V + 2E}{3\mathscr{L}} \tag{10}$$

$$\frac{di_3}{dt} = \frac{2(V + 2E)}{3\mathscr{L}}. \tag{11}$$

Finally, for the sequence of Fig. 5(d), where there are only two phases conducting in series, the derivative of currents i_2 and i_3 is given by

$$\frac{di_2}{dt} = -\frac{di_3}{dt} = \frac{V - 2E}{2\mathscr{L}}. \tag{12}$$

Analysis of Commutation

From the above equations, it is possible to determine the commutation sequence's duration and the condition for the three cases to occur.

Case a: In this case (Fig. 6), $i_1(t_f) = 0$; then, the commutation time t_f can be calculated from (6) as

$$t_f = \frac{3\mathscr{L}I}{V + 2E} \tag{13}$$

but it is also known that $i_2(t_f) = I$; then, from (7)

$$t_f = \frac{3\mathscr{L}I}{2(V - E)}. \tag{14}$$

The condition for case a to take place can be obtained from these two equations and is given by

$$V = 4E. \tag{15}$$

For a constant voltage V at the input of the inverter, this condition corresponds to a given speed.

The commutation duration is given by

$$t_f = \frac{\mathscr{L}I}{2E}. \tag{16}$$

It is to be noted that in this case, the derivative of current i_3 (5) is zero, meaning that this current remains unchanged during commutation.

Case b: In this case, the commutation is made in two sequences (Fig. 7). The first sequence, defined by the time that current i_1 takes to vanish, is characterized by the circuit of Fig. 5(b). The duration of this step is given from (6) by

$$t'_f = \frac{3\mathscr{L}I}{V + 2E}. \tag{17}$$

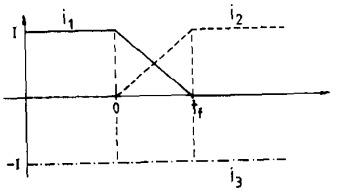

Fig. 6. Case a currents evolution.

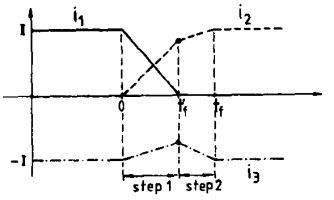

Fig. 7. Case b currents evolution.

At the end of this sequence, current i_2 is given from (7) by

$$i_2(t'_f) = \frac{2(V - E)}{V + 2E}I. \tag{18}$$

The condition for having case b is given by $i_2(t'_f) < I$, that is, from (18)

$$V < 4E. \tag{19}$$

For the second sequence, there are only two phases conducting in series, and the circuit configuration is that of Fig. 5(d).

The total duration of the commutation is given by

$$t_f = \frac{\mathscr{L}I}{V - 2E}. \tag{20}$$

It is important to note that in this case, current i_3, which is not directly involved in the commutation, does not remain constant because its derivative ((5) and (12)) is different from zero when the condition of (19) is fulfilled.

When the duration of commutation t_f becomes greater than $\pi/3\omega$, the current in the machine winding does not reach the reference current I, and then, it is no longer controlled. This limit depends on the value of the current and on the speed.

Case c: In this case, the commutation is also done in two sequences (Fig. 8). The first one corresponds to the circuit of Fig. 5(b) and the second one to the circuit of Fig. 5(c).

From (7), the duration of the first sequence is obtained:

$$t''_f = \frac{3\mathscr{L}I}{2(V - E)}. \tag{21}$$

At the instant t''_f, the current i_1 is given from (9) by

$$i_1(t''_f) = I\left[\frac{V - 4E}{2(V - E)}\right]. \tag{22}$$

The condition for having this situation is given by $i_2(t''_f) = I$ and by $i_1(t''_f) > 0$, that is, from (22):

$$V > 4E. \tag{23}$$

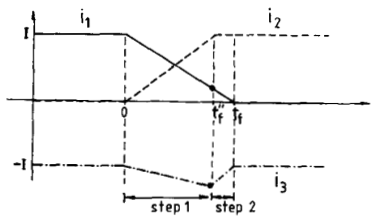

Fig. 8. Case c currents evolution.

From the analysis of the circuit of Fig. 5(c) corresponding to the second sequence ((9) to (11)), it is possible to obtain the total duration t_f of the commutation

$$t_f = \frac{3\mathscr{L}I}{V + 2E}. \tag{24}$$

It is to be noted that in this case, current i_3 also varies because its derivative ((5) and (11)) is different from zero when the condition of (23) is fulfilled. Moreover, the sign of the derivative is inverted with respect to that occurring in case b.

Torque During Commutation

The general expression of torque was given in (2), and the torque between commutation is given by

$$T = \frac{2EI}{\omega}. \tag{25}$$

The first sequence of commutation is common to the three cases analyzed above. The torque during this first sequence is given by

$$T = \frac{1}{\omega}\left[Ei1 + Ei2 - Ei3\right].$$

As $i_1 + i_2 + i_3 = 0$, then

$$T = -\frac{2E}{\omega} i3. \tag{26}$$

This result shows that the torque is proportional to the current not directly involved in the commutation.

Replacing i_3 by the expression of (8) becomes

$$T = \frac{2E}{\omega}\left[I + \frac{V - 4E}{3\mathscr{L}}t\right]. \tag{27}$$

From (25) and (27), it can be seen that during the first sequence, the torque varies as follows:

$V = 4E$ (case a) ⇒ torque remains constant
$V < 4E$ (case b) ⇒ torque decreases
$V > 4E$ (case c) ⇒ torque increases.

To evaluate the torque ripple amplitude during commutation, it is only necessary to calculate its value at the end of the first step, that is, for $V < 4E$ (case b)

$$T(t_f') = \frac{2EI}{\omega}\left[1 + \frac{V - 4E}{V + 2E}\right]. \tag{28}$$

Dividing by (25), the relative torque ripple is obtained:

$$\Delta T = \frac{V - 4E}{V + 2E} \quad \text{(pu)}. \tag{29}$$

For $V > 4E$ (case c)

$$T(t_f'') = \frac{2EI}{\omega}\left[1 + \frac{V - 4E}{2(V - E)}\right]. \tag{30}$$

The relative torque ripple is given by

$$\Delta T = \frac{V - 4E}{2(V - E)} \quad \text{(pu)}. \tag{31}$$

This relation is only valid as long as the current is controlled ($t_f \leq \pi/3\omega$).

Equation (29) and (31) show that for $V = ct$, the relative torque ripple due to the commutation is independent of the current I but depends on the emf E (i.e., of the speed).

Theoretical Results

The relative torque ripple and the duration of the commutation calculated from the above equation for a given machine can be synthesized as in Fig. 9 . The corresponding torque-speed characteristic is given in Fig. 10.

The maximum relative torque ripple reaches +50% at low speed and slopes to −50% at high speed passing by zero for the speed corresponding to $V = 4E$.

The duration of commutation, given in Fig. 9(b), slightly decreases as speed increases in the low-speed range, and it increases rapidly as speed increases in the high-speed range. This duration is minimum for $V = 4E$ when the torque ripple is zero.

The results of Fig. 9 allows explanation of the shape of the torque-speed curve given in Fig. 10. In the low-speed range, in spite of having a large torque ripple amplitude, the effect of commutation on the average torque is not sensible because its duration is small. On the other hand, in the high-speed range, the effect of commutation becomes important because both the duration of commutation and the torque ripple amplitude increases as speed increases.

Control from Direct Phase Currents Sensing

For this control, the current sensors are placed in the ac link between inverter and machine. Only two sensors are needed because the third current can be constructed from the others.

In this control, each inverter branch is commanded from the evolution of the corresponding phase current. For the study of this control, the hypotheses and conditions of the above section are retained.

Commutation Analysis

Starting with phases 1 and 3 supplied, the first commutation sequence always corresponds to Fig. 5(b) and (3) to (8).

According to the above analysis, it is necessary to examine three cases:

Case d ⇒ V = 4E: The derivative of current i_3 is zero; therefore, the hysteresis control related to phase 3 does not operate, and the behavior is the same as in *case a*.

Case e ⇒ V < 4E: During the first sequence of commuta-

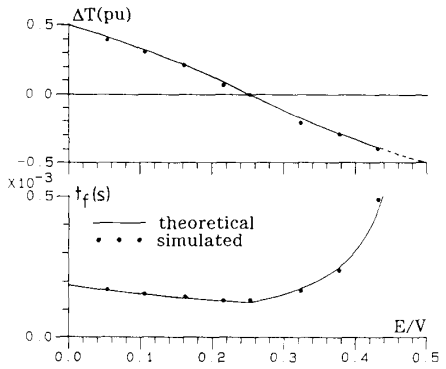

Fig. 9. (a) Relative torque ripple amplitude and (b) its duration.

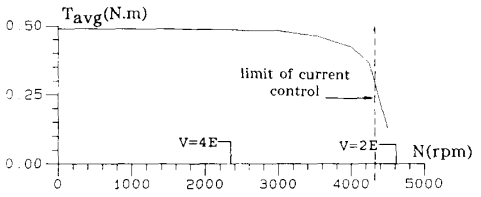

Fig. 10. Torque speed characteristics.

tion, current i_3 is negative, and its derivative is positive; therefore, even with switch $T6$ on, the current i_3 will continue to decrease up to the current i_1 vanishes; the behavior is the same as in *case b*.

Case f ⇒ $V > 4E$: During the first sequence of commutation, the current i_3 is negative, and its derivative is also negative; this means that its amplitude tends to increase. When the upper limit of the hysteresis band is reached, $T6$ is switched off; in the same manner, when current i_3 reaches the lower limit of the hysteresis band, $T6$ is switched on. Therefore, the current i_3 is controlled during the commutation between phases 1 and 2.

Torque Ripple

From the above analysis, the torque ripple in cases d and *e* is the same as in cases a and b. On the other hand, in case f, the commutation of phase current does not introduce torque ripple because the current that is not involved in the commutation (and to which the torque is proportional) is controlled. The torque ripple then corresponds to that introduced by the hysteresis bandwidth. The different cases can be summarized as follows:

- $V = 4E$ ⇒ case d–torque remains constant
- $V < 4E$ ⇒ case e–torque decreases
- $V > 4E$ ⇒ case f–torque ripple corresponds to the hysteresis band.

Simulation and Experimental Results

The above theoretical analysis has been validated by a numerical simulation and illustrated by experimental results.

Simulation Results

A software program was developed to study the behavior of brushless dc motors [7]. It considers a permanent magnet machine with constant synchronous inductances and a trapezoidal emf with a plateau of 120°. The power switches are considered to be ideal, and it is possible to simulate the two ways current is controlled: with dc link current sensing and with ac link current sensing.

The different cases studied in the theoretical analysis have been simulated, and the first results presented concern the evolution of currents and torque for a current control from the dc link. These results are given in Figs. 11 , 12, and 13.

Fig. 11 shows a simulation result in the range of speed where $V > 4E$. As was predicted by the theoretical analysis, torque increases during commutation and is proportional to i_3.

The result obtained for $V = 4E$ is shown in Fig. 12, where it is verified that the torque remains constant during commutation.

Finally, Fig. 13 shows the results for a speed in the range where $V < 4E$. The two sequences of commutation can be clearly identified in this figure, and the theoretical predictions are verified, that is, the torque ripple introduced by the commutation corresponds to a decrease of the average torque.

Beyond this qualitative analysis, the torque ripple and the duration of commutation have been measured from simulation. These results are marked in Figs. 9(a) and (b), corresponding to theoretical results. Because of the good agreement between these results, it can be verified that the main hypothesis taken for the theoretical analysis (hysteresis band neglected and emf constant during commutation) does not affect the results even in the high-speed range.

The last simulation result presented is given in Fig. 14 and concerns the evolution of currents and torque in case of current control by directly sensing the machine currents in the low-speed range. In this figure, it appears, according to the theoretical analysis, that the current not directly involved in the commutation is effectively controlled and that the torque ripple during commutation is proportional to the ripple of this current.

In the high-speed range, the results obtained with this control are the same as in Figs. 11 and 12.

Experimental Verification

In order to present experimental results to illustrate the theoretical and simulation ones, some tests were made on a brushless dc motor that was available in the laboratory. This drive consists of a machine with magnets associated with polar pieces fed by a MOSFET inverter.

Fig. 15 shows the experimental result obtained using an hysteresis control and dc link current sensing. Fig. 15(a) was obtained in the low-speed range and is quite comparable with Fig. 9. Fig. 15(b) was obtained almost at the speed corresponding to $V = 4E$ and is also comparable with Fig. 10. Finally, Fig. 15(c) corresponds to a speed in the range where $V < 4E$ and is comparable with Fig. 11.

It should be noted that these results have been obtained on a machine with salient poles whose inductance varies with rotor position, which is contrary to the model used here. Nevertheless, they confirm the validity of the main conclusions obtained, and beyond this, they indicate that they can be generalized to other kinds of permanent magnet machines.

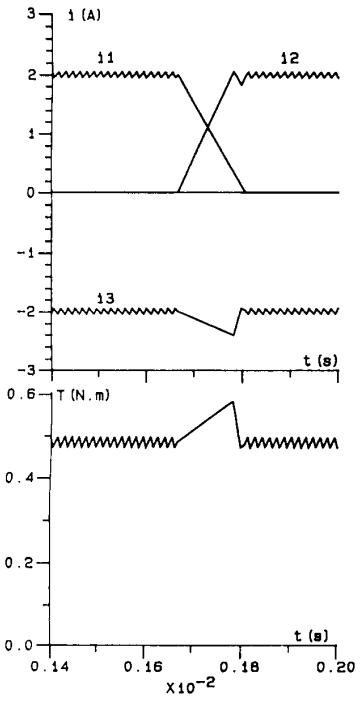

Fig. 11. Simulated result with dc link current sensing for $V > 4E$.

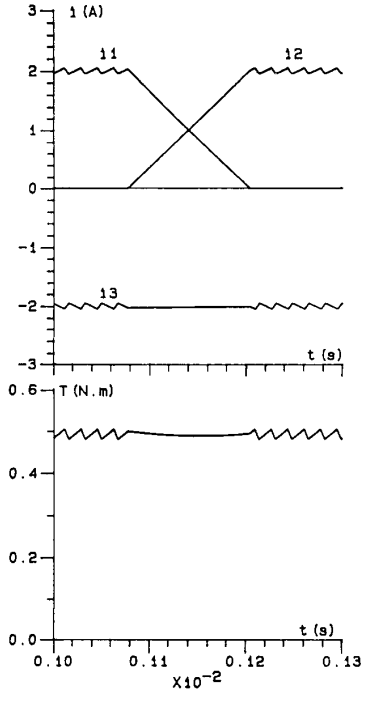

Fig. 12. Simulated result with dc link current sensing for $V = 4E$.

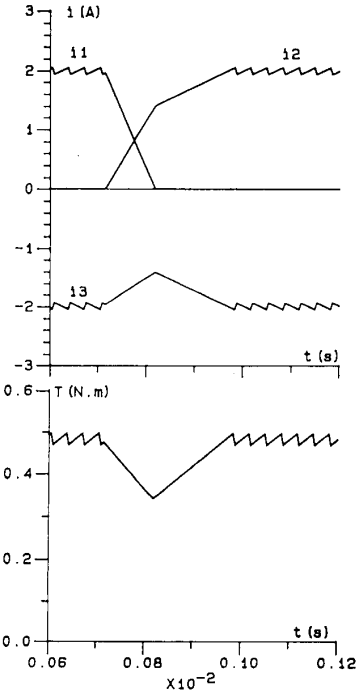

Fig. 13. Simulated result with dc link current sensing for $V < 4E$.

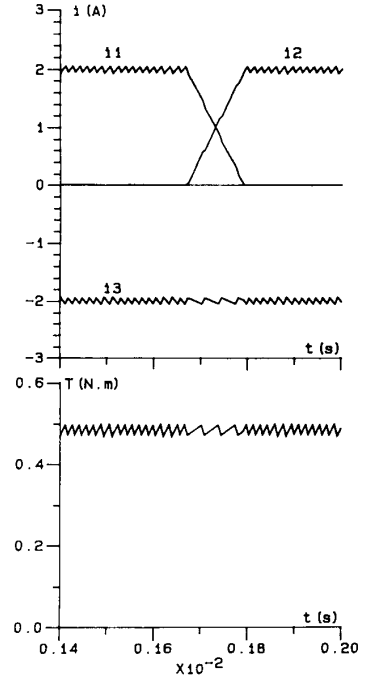

Fig. 14. Simulated results with direct phase current sensing for $V > 4E$.

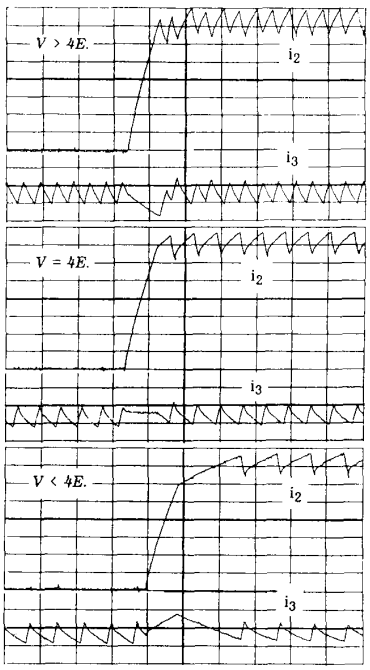

Fig. 15. Simulated results.

Another generalization has been made using a PWM dc link current control instead of the hysteresis control used in this analysis (for simplification reasons). The experimental analysis made shows that with PWM control, the conclusions are practically the same as those presented here with hysteresis control.

Conclusions

This paper has presented an analytical study of torque ripple due to commutation of phase currents in a brushless dc motor. The results have been validated by simulation and illustrated by tests. The results indicate that in the range where the current is effectively controlled, the relative ripple is independent of current, varies with the speed, reaches 50% of the average torque at very low speed, and slopes to -50% at high speed. Particular attention was also paid to the duration of the commutation, which becomes very important with respect to the electrical period in the high-speed range.

Two kinds of current control have been analyzed. The first one, based on the dc link sensing, has the advantage of simplicity, but the second one, based on direct machine current sensing, allows elimination of the torque pulsation due to commutation in the lower speed range. When this duration becomes greater than one sixth of the electrical period, the current is no longer controlled.

From this analysis, it is possible to get the influence of the machine inductance, and then, this can be introduced in the machine design in order to minimize the influence of commutation.

References

[1] T. Li and G. Slemon, "Reduction of cogging torque in permanent magnet motors," *IEEE Trans. Magn.*, vol. EC-2, no. 6, Nov. 1988.

[2] R. Carlson, A. A. Tavares, J. P. Bastos, and M. Lajoie-Mazenc, "Torque ripple attenuation in permanent magnet synchronous motors," in *Conf. Rec. 1989 IEEE IAS Ann. Mtg.* (San Diego, CA), Oct. 1-5, 1989, pp. 57-62.

[3] M. Lajoie-Mazenc, B. Nogarede, and J. C. Fagundes, "Analysis of torque ripple in electronically commutated permanent magnet machines and minimization methods," in *Conf. Rec. Fourth Int. Conf. Elect. Machines Drives* (London), Sept. 13-15, 1989, pp. 85-89.

[4] P. Pillay and R. Krishnan, "Modeling, simulation, and analysis of a permanent magnet brushless dc motor drive," in *Conf. Rec. 1987 IEEE IAS Ann. Mtg.* (San Diego, CA), Oct. 1-5, 1989, pp. 7-14.

[5] M. Lajoie-Mazenc, J. Cros, and M. Cartignies, "Vers l'intégration mécatronique: la commande sans capteur des machines à aimants sans balais," *Revue SIA Ingénieurs de l'Automobile*, no. 660, Oct. 1990.

[6] T. J. E. Miller, *Brushless Permanent Magnet and Reluctance Motor Drives*. Oxford: Clarendon, 1989.

[7] R. Carlson, A. A. Tavares, and M. Lajoie-Mazenc, "Operating analysis and simulation of a brushless dc machine with a 120° hysteresis current controlled voltage inverter," in *Conf. Rec. 3rd Euro. Conf. Power Electron. Applications* (Aachen), Oct. 9-12, 1989, pp. 1507-1511.

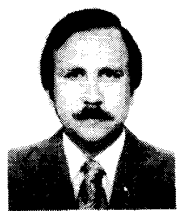

Renato Carlson (M'79) was born in Porto Alegre, Brazil, in 1943. He received the Engineering degree in 1969 from Universidade Federal do Rio Grande do Sul and the M.Sc. degree in 1973 from Universidade Federal de Santa Catarina (UFSC), Brazil. He received the Doctor degree from Universite Paul Sabatier, France, in 1976.

Since 1970, he has been with the Department of Electrical Engineering of UFSC. Since 1981, he has been a Full Professor. He is presently Head of his Department. His fields of interest include the design of permanent-magnet machines with electronic commutation, ac drives, and power electronics.

Michel Lajoie-Mazenc was born in Decazeville, France, in 1938. He joined the Laboratoire d'Electrotechnique et d'Electronique Industrielle (LEEI), Toulouse, in 1965 and received the Doctorat d'Etat degree from the University Paul Sabatier in 1969.

He is presently "Directeur de Recherche au Centre National de la Recherche Scientifique (CNRS)" and has been Head of the LEEI since 1987. His field of interest is the modelization, design, and testing of electronically commutated permanent-magnet machines.

Joao C. dos S. Fagundes was born in Osorio, Brazil, in 1954. He received the Engineering degree in 1980, from Universidade Federal do Rio Grande do Sul and the M.Sc. Degree in 1983, from Universidade Federal de Santa Catarina (UFSC), Brazil. He received the Doctor degree from Institut National Polytechnique, Toulouse, France, in 1990.

Since 1982, he has been a Professor with the Department of Electrical Engineering, UFSC. His fields of interest include power electronics and ac drives.